Cellular/Molecular

Mutation of Glutamate 155 of the $GABA_A$ Receptor β_2 Subunit Produces a Spontaneously Open Channel: A Trigger for Channel Activation

J. Glen Newell, Ross A. McDevitt, and Cynthia Czajkowski
Department of Physiology, University of Wisconsin, Madison, Wisconsin 53706

Protein movements underlying ligand-gated ion channel activation are poorly understood. The binding of agonist initiates a series of conformational movements that ultimately lead to the opening of the ion channel pore. Although little is known about local movements within the GABA-binding site, a recent structural model of the $GABA_A$ receptor ($GABA_AR$) ligand-binding domain predicts that β_2Glu^{155} is a key residue for direct interactions with the neurotransmitter (Cromer et al., 2002). To elucidate the role of the β_2Ile^{154}–Asp^{163} region in $GABA_AR$ activation, each residue was individually mutated to cysteine and coexpressed with wild-type α_1 subunits in *Xenopus laevis* oocytes. Seven mutations increased the GABA EC_{50} value (8- to 3400-fold), whereas three mutations (E155C, S156C, and G158C) also significantly increased the 2-(3-carboxypropyl)-3-amino-6-(4-methoxyphenyl) pyridazinium (SR-95531) K_I value. GABA, SR-95531, and pentobarbital slowed *N*-biotinylaminoethyl methanethiosulfonate modification of T160C and D163C, indicating that β_2Thr^{160} and β_2Asp^{163} are located in or near the GABA-binding site and that this region undergoes structural rearrangements during channel gating. Cysteine substitution of β_2Glu^{155} resulted in spontaneously open $GABA_ARs$ and differentially decreased the GABA, piperidine-4-sulfonic acid (partial agonist), and SR-95531 sensitivities, indicating that the mutation perturbs ligand binding as well as channel gating. Tethering thiol-reactive groups onto β_2E155C closed the spontaneously open channels, suggesting that β_2Glu^{155} is a control element involved in coupling ligand binding to channel gating. Structural modeling suggests that the β_2 Ile^{154}–Asp^{163} region is a protein hinge that forms a network of interconnections that couples binding site movements to the cascade of events leading to channel opening.

Key words: **GABA; SR-95531; gabazine; picrotoxin; piperidine-4-sulfonic acid; mutagenesis; substituted cysteine accessibility method; pentobarbital; *Xenopus laevis* oocytes; methanethiosulfonate; two-electrode voltage clamp**

Introduction

Agonists and antagonists induce different molecular rearrangements in neurotransmitter-binding sites of ligand-gated ion channels (LGICs) (Armstrong and Gouaux, 2000; Boileau et al., 2002; Chang and Weiss, 2002). Agonists, but not antagonists, promote opening of the ion channel pore. It is likely that movements of amino acids near or within the neurotransmitter recognition site trigger the cascade of events leading to channel opening (Boileau et al., 2002; Torres and Weiss, 2002; Unwin et al., 2002; Miyazawa et al., 2003; Chakrapani et al., 2004). Here, we examined the I1e^{154}–Asp^{163} region of the $GABA_A$ receptor ($GABA_AR$) β_2 subunit to identify residues that mediate local movements within the binding site that initiate channel gating and residues involved in GABA binding.

$GABA_ARs$ are heteropentameric LGICs that mediate fast synaptic inhibitory neurotransmission in the brain. The $\alpha_1\beta_2\gamma_2$ $GABA_AR$ subtype is the most abundant *in vivo*, and heterologous expression studies suggest a β-α-β-α-γ stoichiometry and subunit arrangement (Chang et al., 1996; Tretter et al., 1997; Farrar et al., 1999; Baumann et al., 2001, 2002). Expression of α and β subunits also gives rise to functional $GABA_AR$ with putative stoichiometries of either 3α:2β (Im et al., 1995) or 3β:2α (Baumann et al., 2001; Horenstein et al., 2001) that lack sensitivity to benzodiazepines (Schofield et al., 1987; Pritchett et al., 1989), are responsive to barbiturates, and have a high apparent affinity for agonists (Boileau et al., 1999, 2002; Wagner and Czajkowski, 2001).

A recent homology model of the $GABA_AR$ agonist-binding site predicts that β_2Glu^{155} interacts with the positively charged moiety of GABA (Cromer et al., 2002). In addition, mutagenesis studies have determined that nearby residues, β_2Tyr^{157} and β_2Thr^{160}, are important for GABA binding (Amin and Weiss, 1993). Similarly, amino acid residues in aligned regions of the muscle-type nicotinic acetylcholine α1 (Trp^{148}, Tyr^{151}, and Asp^{152}) (Dennis et al., 1988; Galzi et al., 1991; Sugiyama et al., 1996), glycine α1 (Asp^{148}, Gly^{160}, and Tyr^{161}) (Vandenberg et al.,

Received Sept. 9, 2004; revised Nov. 1, 2004; accepted Nov. 1, 2004.

This work was supported by National Institute of Neurological Disorders and Stroke Grant 34727 to C.C. and a Postdoctoral Fellowship from the Natural Sciences and Engineering Research Council of Canada to J.G.N.

Correspondence should be addressed to Cynthia Czajkowski, Department of Physiology, University of Wisconsin–Madison, 601 Science Drive, Madison, WI 53711. E-mail: czajkowski@physiology.wisc.edu.

J. G. Newell's present address: Department of Physiology, University of Toronto, Room 3318, Medical Sciences Building, 1 King's College Circle, Toronto, Ontario, Canada M5S 1A8.

R. A. McDevitt's present address: Graduate Program in Neurobiology and Behavior, University of Washington, Box 357270, Room T-471, Seattle, WA 98195.

DOI:10.1523/JNEUROSCI.3746-04.2004

 0270-6474/04/2411226-10$15.00/0

1992, 1993), and serotonin type 3 receptor subunits (Trp^{160}) (Spier and Lummis, 2000) have been determined to be critical for agonist–antagonist binding (see Fig. 1) and define region "B"[a] of the ligand-binding site. The contributions of these residues in forming their respective agonist binding sites are supported by homology models that place this region (from β-strand 7 and loop 8) within the putative core of LGIC neurotransmitter-binding sites (Cromer et al., 2002; Holden and Czajkowski, 2002; LeNovère et al., 2002; Newell and Czajkowksi, 2003; Reeves et al., 2003).

Here, we demonstrate that expression of $\alpha_1\beta_2$(E155C) gives rise to spontaneously open GABA channels. Mutation of β_2Glu^{155} alters both channel-gating properties and impairs agonist binding. In addition, we provide evidence that β_2Thr^{160} and β_2Asp^{163} are found on an aqueous surface within or near the GABA-binding site and undergo conformational rearrangements during pentobarbital-mediated gating events. Together, the data suggest that movement in this region of the GABA-binding site is one of the initial triggers for coupling binding to gating.

Materials and Methods

Mutagenesis and expression in oocytes. Rat cDNAs encoding the $GABA_AR$ α_1 and β_2 subunits were used in this study. The β_2 cysteine mutants were engineered using a recombinant PCR method, as described previously (Boileau et al., 1999; Kucken et al., 2000). Cysteine substitutions were made in the β_2 subunit at Ile^{154}, Glu^{155}, Ser^{156}, Tyr^{157}, Gly^{158}, Tyr^{159}, Thr^{160}, Thr^{161}, Asp^{162}, and Asp^{163} (see Fig. 1). Cysteine substitutions were verified by restriction endonuclease digestion and double-stranded DNA sequencing.

All wild-type and mutant cDNAs were subcloned into the vector pGH19 (Liman et al., 1992; Robertson et al., 1996) for expression in *Xenopus laevis* oocytes. Oocytes were isolated as described previously (Boileau et al., 1998). cRNA transcripts were prepared using the T7 mMessage machine (Ambion, Austin, TX). $GABA_A$ receptor α_1 and β_2 or β_2 mutant subunits were coexpressed by injection of cRNA (675 pg/subunit) in a 1:1 ratio (α:β). The oocytes were maintained in modified ND96 medium [containing (in mM): 96 NaCl, 2 KCl, 1 $MgCl_2$, 1.8 $CaCl_2$, and 5 HEPES, pH 7.4] that had been supplemented with 100 μg/ml gentamicin and 100 μg/ml bovine serum albumin. Oocytes were used 2–7 d after injection for electrophysiological recordings.

Two-electrode voltage-clamp analysis. Oocytes under two-electrode voltage clamp were perfused continuously with ND96 recording solution [containing (in mM): 96 NaCl, 2 KCl, 1 $MgCl_2$, 1.8 $CaCl_2$, 5 HEPES, pH 7.4] at a rate of ~5 ml/min. The holding potential was −80 mV. The volume of the recording chamber was 200 μl. Standard two-electrode voltage-clamp procedures were performed using a GeneClamp500 Amplifier (Axon Instruments, Foster City, CA). Borosilicate electrodes were filled with 3 M KCl and had resistances of 0.5–3.0 MΩ in ND96. Stock solutions of GABA, 2-(3-carboxypropyl)-3-amino-6-(4-methoxyphenyl) pyridazinium (SR-95531) and piperidine-4-sulfonic acid (P4S) (Sigma, St. Louis, MO) were prepared in water, whereas stock solutions of picrotoxin (PTX) (Sigma) and *N*-biotinylaminoethyl methanethiosulfonate (MTSEA-biotin; 100 mM; Biotium, Hayward, CA) were prepared in dimethylsulfoxide (DMSO). All compounds were diluted appropriately in ND96 such that the final concentration of DMSO was ≤2%. The vehicle did not affect GABA-activated currents.

To measure the sensitivity to GABA or P4S, the agonist (0.0001–100 mM) or partial agonist (0.00001–10 mM) was applied via gravity perfusion or by pipette application (~5–8 sec) with a 3–15 min washout period between each application to ensure complete recovery from desensitization. Peak GABA- or P4S-activated current (I_{GABA} or I_{P4S}) was recorded. To correct for slow drift in the amplitude of the response as a function of time, concentration–response data were normalized to a low concentration of agonist (EC_2–EC_5). The apparent affinity of pentobarbital using concentrations between 0.01 and 10 mM was determined via gravity perfusion (~5–8 sec) with a 3–5 min washout period between each application. Peak pentobarbital-activated current was recorded. Concentration–response data for pentobarbital were normalized to a previous application of pentobarbital (100 μM). Concentration–response curves for GABA, P4S, or pentobarbital were generated for each recombinant receptor, and the data were fitted by nonlinear regression analysis using Prism software (GraphPad, San Diego, CA). Data were fitted to the following equation: $I = I_{max}/(1 + (EC_{50}/[A])^n)$, where I is the peak amplitude of the current for a given concentration of GABA, P4S, or pentobarbital ($[A]$), I_{max} is the maximum current, EC_{50} is the concentration required for half-maximal receptor activation, and n is the Hill coefficient.

To determine SR-95531 or PTX IC_{50} values, GABA (EC_{50}) was applied via gravity perfusion followed by a brief washout period (20 sec) before application of GABA (EC_{50}) and increasing concentrations of SR-95531 or PTX. The response to the application of SR-95531/PTX and GABA was normalized to the response elicited by the agonist alone. Concentration–inhibition curves were generated by nonlinear regression analysis using GraphPad Prism software. Data were fitted to the following equation: $1 - 1/(1 + (IC_{50}/[Ant])^n)$, where IC_{50} is the concentration of antagonist ($[Ant]$) that reduces the amplitude of the GABA-evoked current by 50%, and n is the Hill coefficient. SR-95531 K_I values were calculated using the Cheng–Prussof correction: $K_I = IC_{50}/(1 + ([A]/EC_{50}))$, where $[A]$ is the concentration of GABA used in each experiment, and EC_{50} is the concentration of GABA that elicits a half-maximal response for each receptor (Cheng and Prussof, 1973).

Modification of cysteine residues by MTSEA-biotin. MTSEA-biotin was the cysteine-specific reagent used in this study because it is a relatively impermeant compound (Daniels and Amara, 1998), the dimensions (14.5 Å unreacted moiety; 11.2 Å reacted moiety) of which are similar to SR-95531 (13.5 Å) but longer than GABA (4.5 Å). Therefore, it is reasonable to assume that MTSEA-biotin can occupy the GABA-binding site and that this reagent will principally modify extracellular cysteine residues. We used the following criterion for stability of the response for these studies: ≤10% variation in I_{GABA} (EC_{50}) on two consecutive applications at regular intervals (10 min). Oocytes were then allowed to recover fully, after which a high concentration of MTSEA-biotin (2 mM) was applied (2 min). After MTSEA-biotin application, cells were washed (5 min) with ND96, after which GABA (EC_{50}) was reapplied to determine the effect of MTSEA-biotin application on I_{GABA}. Effects of MTSEA-biotin were calculated as the difference in the amplitude of the GABA-gated current before and after MTSEA-biotin application as follows: $(I_{GABAPRE} - I_{GABAPOST}/I_{GABAPRE}) \times 100$, where "post" refers to the amplitude of the GABA-gated current after MTSEA-biotin application, and "pre" refers to the amplitude of the stabilized GABA-gated current before covalent modification by MTSEA-biotin.

Rate of MTSEA-biotin reaction. The rate at which MTSEA-biotin modified introduced cysteine residues (E155C, T160C, and D163C) was measured using low MTSEA-biotin concentrations, as described previously (Newell and Czajkowski, 2003). The concentrations of MTSEA-biotin used were 50 nM (D163C), 100 nM (T160C), and 2 mM (E155C). The experimental protocol is described as follows: GABA (EC_{50}) application (5 sec), ND96 washout (25 sec), MTSEA-biotin application (10–20 sec), ND96 washout (2.2–2.3 min). The sequence was repeated until I_{GABA} no longer changed after the MTSEA-biotin treatment (i.e., the reaction had proceeded to apparent completion). The individual abilities of GABA, SR-95531, and pentobarbital to alter the rate of cysteine modification by MTSEA-biotin were determined by coapplying GABA ($5 \times EC_{50}$), SR-95531 ($6 \times K_I$), or pentobarbital (50 or 500 μM) during the MTSEA-biotin pulse. In all cases, the wash times were adjusted to ensure that currents obtained from test pulses of GABA (EC_{50}) after exposure to high concentrations of GABA, SR-95531, or pentobarbital were stable. This ensured (1) a complete washout of drugs and that (2) reductions in the current amplitude resulted from the application of MTSEA-biotin.

For all rate experiments, the decrease in I_{GABA} was plotted as a function

[a]Throughout this paper, the six previously identified binding site regions are named by the letters A–F (Galzi and Changeux, 1994; Lester et al., 2004). Based on the structure of AChBP (Brejc et al., 2001), these regions can be defined as follows: region A, β strand 4 and loop 5; region B, β strand 7 and loop 8; region C, β strand 9, loop 10 and β strand 10; region D, β strand 2; region E, β strands 5′ and 6; region F, loop 9. When we refer to regions that are not part of the binding site, these are named by numbers based on AChBP structure.

of the cumulative time of MTSEA-biotin exposure and fit to a single-exponential decay function using GraphPad Prism software. A pseudo-first-order rate constant (k_1) was determined, and the second-order rate constant (k_2) was calculated by dividing k_1 by the concentration of MTSEA-biotin used in the assay (Pascual and Karlin, 1998). Second-order rate constants were determined using at least two different concentrations of MTSEA-biotin to ensure accuracy of the protocol.

Statistical analysis. Log (EC_{50}) values, log (K_I) values, and log (k_2) rates were analyzed using a one-way ANOVA followed by a Dunnett's *post hoc* test to determine levels of significance.

Structural modeling. The mature protein sequences of the rat α_1 and β_2 subunits were homology modeled with a subunit of the ACh binding protein (AChBP) (Brejc et al., 2001). The crystal structure of the AChBP was downloaded from RCSB Protein Data Bank (code 1I9B) and loaded into Swiss Protein Bank Viewer (SPDBV). The α1 protein sequence from Thr^{12}–Ile^{227} and the β_2 protein sequence from Ser^{10}–Leu^{218} were aligned with the AChBP primary amino acid sequence as depicted by Cromer et al. (2002) and threaded onto the AChBP tertiary structure using the "Interactive Magic Fit" function of SPDBV. The threaded subunits were imported into SYBYL (Tripos, St. Louis, MO), in which energy minimization was performed (<0.5 kcal/Å). The first 100 iterations were performed using Simplex minimization (Press et al., 1988) followed by 1000 iterations using the Powell conjugate gradient method (Powell, 1977). A β_2/α_1 GABA-binding site interface was assembled by overlaying the monomeric subunits on the AChBP scaffold, and the resulting structure was imported into SYBYL and energy minimized. Neither water nor entropy factors were included during the minimizations. After the global energy minimization, several TRIPOS programs were run to evaluate the accuracy of the model. Ramachandran plots, χ plots, side-chain positions, and *cis*- and *trans*-bonds were all examined. Problems in the structure that were revealed by these evaluations were fixed manually, and energy minimizations were run again as needed. Our model is quite similar to models published recently for the nicotinic ACh receptor (nAChR) and $GABA_A$R ligand-binding domains (Cromer et al., 2002; LeNovère et al., 2002). Regions with insertions were modeled by fitting structures from a loop database. Because the sequence identity of the AChBP and the $GABA_A$R extracellular ligand-binding domain is only 18%, caution must be used in interpreting the absolute positions of individual side-chain residues in the model.

Results

Expression and functional characterization of cysteine mutants

Cysteine substitutions were engineered at 10 individual positions (Fig. 1) in the $GABA_A$R β_2 subunit (Ile^{154}, Glu^{155}, Ser^{156}, Tyr^{157}, Gly^{158}, Tyr^{159}, Thr^{160}, Thr^{161}, Asp^{162}, and Asp^{163}), coexpressed with wild-type α_1 subunits in *X. laevis* oocytes, and analyzed using two-electrode voltage clamp. Expression of most mutant β_2 subunits produced functional channels (I_{GABA} = 1–10 μA), with the exceptions Y157C and Y159C. We speculate that introduction of cysteine residues at these positions impaired assembly of mutant receptors.

For the cysteine mutants that did express, seven of eight significantly increased GABA EC_{50} values, demonstrating that this region is particularly sensitive to structural perturbation. Expression of receptors containing I154C, E155C, S156C, G158C, T160C, D162C, and D163C increased GABA EC_{50} values 8-, 3375-, 22-, 260-, 23-, 18-, and 9-fold relative to wild type (1.6 μM) (Fig. 2*A*, Table 1). The Hill coefficients for GABA activation of G158C- and D163C-containing receptors were significantly lower than wild type.

		154	155	156	157	158	159	160	161	162	163
$GABA_AR$	β2	I	E	S	Y	G	Y	T	T	D	D
nAChR	α	L	G	I	W	T	Y	D	G	T	K
GlyR	α1	L	D	S	F	G	Y	T	M	N	D
$5HT_3R$	a	P	T	S	W	L	H	T	I	Q	D
AChBP		I	G	S	W	T	H	H	S	R	E

Figure 1. The Ile^{154}–Asp^{163} segment (region B) of the rat $GABA_A$R β_2 subunit is aligned with homologous segments of the *Torpedo* nAChR α, glycine receptor (GlyR) α_1, and 5-HT_{3a} subunits. The numbering reflects the position of the residues in the mature $GABA_A$R β_2 subunit. Circled residues β_2Tyr^{157} and β_2Thr^{160} are implicated in GABA binding (Amin and Weiss, 1993). Residues important for ligand recognition in other binding sites are boxed. nAChR αTrp^{149} and possibly Tyr^{151} and Asp^{152} have been implicated in forming the acetylcholine-binding site (Dennis et al., 1988; Galzi et al., 1991; Sugiyama et al., 1996). GlyR α_1Gly^{160}, Tyr^{161} (Vandenberg et al., 1992; Schmieden et al., 1993), and Phe^{159} (Schmieden et al., 1993) are important for antagonist recognition, whereas 5-HT_{3a} Trp^{160} (Spier and Lummis, 2000) is important for the actions of serotonin. nAChR αG158S has been reported as a naturally occurring mutation in myasthenia gravis patients that gives rise to "slow channels" (Sine et al., 1995; Croxen et al., 1997) $GABA_A$R β_2 subunit residues accessible to MTSEA-biotin modification are underlined (E155C, G158C, T160C, and D163C).

The K_I values for the competitive antagonist SR-95531 were significantly different from wild type (K_I = 163 nM) for E155C, S156C, and G158C by 11-, 3-, and 18-fold, respectively (Table 1, Fig. 2*B*). Small currents (I_{max} < 90 nA) of receptors containing G158C precluded additional analysis.

Pentobarbital is a barbiturate that exerts its pharmacological effects (allosteric modulation and channel opening) via interactions with the $GABA_A$ receptor at a binding site distinct from the GABA site (Akk and Steinbach, 2000). Pentobarbital is therefore useful for assessing the consequences of mutating residues located near the GABA-binding site on overall receptor structure–function. Pentobarbital activated wild-type receptors with an EC_{50} of 1.1 ± 0.3 mM (n = 4) (Table 2) but failed to elicit current in receptors containing Y157C or Y159C, again suggesting that these mutant β_2 subunits did not assemble into functional channels. Sensitivity to pentobarbital was increased approximately twofold for E155C- and T160C-containing receptors [EC_{50} values = 0.53 ± 0.1 mM (n = 4) and 0.32 ± 0.03 mM (n = 3), respectively], whereas expression of D163C (EC_{50} = 2.0 ± 0.3 mM; n = 3) had no significant effect on pentobarbital EC_{50}. These data suggest that the rightward GABA EC_{50} shifts (Table 1) measured for E155C-, T160C-, and D163C-containing receptors are attributable to local effects at the GABA-binding site.

Although it is impossible to know whether the introduced cysteine residues occupy positions equivalent to wild-type resi-

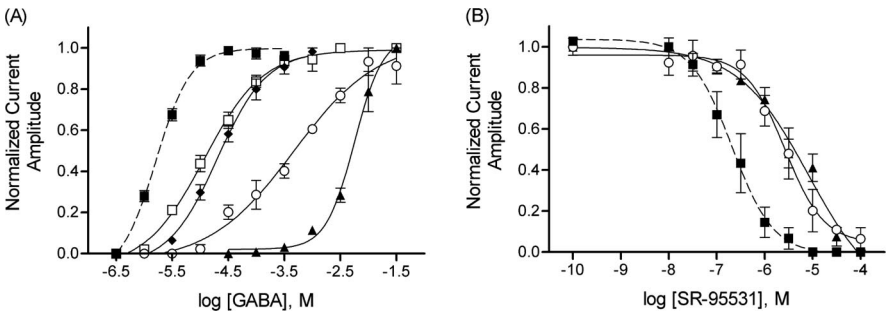

Figure 2. *A*, Concentration–response curves of GABA-activated current for wild type (■), E155C (▲), G158C (○), T160C (◆), and D163C (□) expressed in *Xenopus* oocytes. Data were normalized to peak I_{GABA} for each experiment. Data points represent the mean ± SE of three to five independent experiments. *B*, Concentration dependence of SR-95531 inhibition of I_{GABA} (EC_{50}) current for wild type (■), G158C (○), and E155C (▲). Data points represent the mean ± SE of three independent experiments. The GABA EC_{50} values, SR-95531 K_I values, and calculated Hill coefficients are reported in Table 1.

Table 1. Concentration–response data for GABA activation and SR-95531 inhibition of wild-type and mutant receptors expressed in *Xenopus* oocytes

	GABA				SR-95531			
Receptor	EC_{50} (μM)	n_H	n	mut/wt	K_I (nM)	n_H	n	mut/wt
$\alpha_1\beta_2$	1.6 ± 0.2	1.35 ± 0.15	5	1	163 ± 83	1.13 ± 0.10	3	1
$\alpha_1\beta_2$(I154C)	12.1 ± 4.7**	1.13 ± 0.22	3	7.6	143 ± 63	0.87 ± 0.10	3	0.9
$\alpha_1\beta_2$(E155C)	5400 ± 1500**	1.21 ± 0.07	3	3375	1810 ± 401*	0.66 ± 0.10	3	11.1
$\alpha_1\beta_2$(S156C)	34.5 ± 8.8**	1.32 ± 0.15	3	22	561 ± 178*	0.76 ± 0.15	3	3.4
$\alpha_1\beta_2$(Y157C)	No current							
$\alpha_1\beta_2$(G158C)	416 ± 184**	0.65 ± 0.09**	3	260	2920 ± 1100*	1.35 ± 0.40	3	17.9
$\alpha_1\beta_2$(Y159C)	No current							
$\alpha_1\beta_2$(T160C)	37.4 ± 11.7**	1.40 ± 0.10	6	23	250 ± 88	1.03 ± 0.09	3	1.5
$\alpha_1\beta_2$(T161C)	1.8 ± 0.4	1.10 ± 0.14	3	1.1	132 ± 38	1.03 ± 0.06	3	0.8
$\alpha_1\beta_2$(D162C)	28.5 ± 5.6**	1.48 ± 0.13	4	18	187 ± 115	1.49 ± 0.7	3	1.1
$\alpha_1\beta_2$(D163C)	13.8 ± 3.8*	0.82 ± 0.05*	3	8.6	120 ± 32	0.84 ± 0.12	3	0.7

Data represent the mean ± SE for three to six experiments (n). EC_{50} values, K_I values, and Hill slopes (n_H) were determined from concentration–response data using nonlinear regression analysis with GraphPad Prism software. Hill slopes, log(EC_{50}), and log(K_I) values were analyzed using a one-way ANOVA followed by a Dunnett's test to determine the levels of significance (*$p < 0.05$; **$p < 0.01$; from wild type). mut, Mutant; wt, wild type.

Table 2. Concentration–response data for GABA, P4S, SR-95531, PTX, and pentobarbital for $\alpha_1\beta_2$ and $\alpha_1\beta_2$(E155C) receptors expressed in *Xenopus* oocytes

	$\alpha_1\beta_2$		$\alpha_1\beta_2$(E155C)		
Ligand	EC_{50}/IC_{50} (μM)	n_H	EC_{50}/IC_{50} (μM)	n_H	mut/wt
GABA[a]	1.6 ± 0.2	1.35 ± 0.15	5400 ± 1500*	1.21 ± 0.07	3375
P4S	4.7 ± 0.4	1.59 ± 0.22	730.7 ± 52.1*	1.30 ± 0.11	152
SR-95531[a]	0.2 ± 0.08	1.13 ± 0.10	1.8 ± 0.4*	0.66 ± 0.1	11.1
PTX	4.7 ± 1.2	0.84 ± 0.02	3.1 ± 0.1	0.81 ± 0.10	0.6
Pentobarbital	1100 ± 300	1.56 ± 0.07	530 ± 100*	1.08 ± 0.02	0.5

Data represent the mean ± SE for more than three experiments. EC_{50} values, IC_{50} values, K_I values, and Hill slopes (n_H) were determined from concentration–response data using nonlinear regression analysis with GraphPad Prism software. Hill slopes, log(EC_{50}), log(IC_{50}), and log (K_I) values were analyzed using a two-tailed unpaired t test to determine the levels of significance (*$p < 0.01$; from $\alpha_1\beta_2$). mut, Mutant, wt, wild type.

[a]Values are from Table 1.

dues, because SR-95531 and pentobarbital apparent affinities were similar or, in certain cases, more potent for some mutant receptors in which there were large rightward shifts in GABA EC_{50}, we believe gross structural reorganizations of the $GABA_A$ receptor did not occur as a result of these mutations.

Spontaneous openings at $\alpha_1\beta_2$(E155C)

Expression of $\alpha_1\beta_2$(E155C) receptors gave rise to higher than normal resting conductances (I_{leak}), the magnitudes of which (−609 ± 76 nA; $n = 9$) were ~12-fold greater than injection-matched wild-type receptors (−51 ± 9 nA; $n = 9$). To determine the nature of this high resting conductance, we applied the $GABA_A$R channel blocker PTX. PTX (100 μM) reduced I_{leak} by 72.1 ± 4.2% ($n = 3$) (Fig. 3*A*), demonstrating that spontaneously open $GABA_A$R channels accounted for the high resting conductance. PTX inhibited GABA-activated currents elicited from $\alpha_1\beta_2$(E155C) receptors with an IC_{50} value of 3.1 μM, which was not significantly different from wild-type receptor values (4.7 μM) (Fig. 3*B–D*, Table 2).

Spontaneously active LGICs often arise as a consequence of mutations in the M2 channel-lining segment, and a characteristic of these constitutively open channels is a leftward shift in agonist concentration responses (Bertrand et al., 1992; Filatov and White, 1995; Labarca et al., 1995; Tierney et al., 1996; Chang and Weiss, 1998, 1999; Thompson et al., 1999; Findlay et al., 2000). However, this was not the case on expression of β_2E155C, wherein we observed a 3375-fold decrease in GABA sensitivity. The sensitivity of the partial agonist (P4S) was also reduced (with no apparent reduction in efficacy) (Fig. 4*A*,*B*), albeit to a lesser extent than that of GABA (152-fold) (Table 2, Fig. 4*C*). The mutation also decreased the sensitivity of the competitive antagonist SR-95531 (11.1-fold rightward shift) (Table 2). Again, it should be noted that for this mutation, pentobarbital sensitivity was increased twofold relative to wild type (Table 2, Fig. 4*D*). Mutation of ρ_1Y102 located in the $GABA_C$ receptor D region of the agonist binding site (i.e., β-strand 2) has also been reported to result in spontaneously open channels with similar properties (Torres and Weiss, 2002).

Alterations in EC_{50} values are difficult to evaluate because changes in either ligand binding and/or channel gating can alter this macroscopic constant (Colquhoun, 1998). The increase in open probability for the E155C mutant indicates that the mutation altered $GABA_A$ receptor channel gating. If the mutation altered gating exclusively, similar-fold changes in the apparent affinities of a series of ligands as well as leftward shifts in their concentration responses would be expected (Zhang et al., 1994). The apparent affinities for GABA, P4S, and SR-95531 were altered by different factors (Table 2), and rightward shifts in their concentration responses were observed. Thus, these data indicate that, besides altering gating, E155C decreased the binding of orthosteric ligands to the GABA-binding site. We can exclude the possibility that these differential effects arise from a mixed population of receptors [i.e.,$\alpha_1\beta_2$(E155C) and β_2(E155C)] because expression of β_2E155C alone produced no currents.

In addition to PTX, covalent modification of E155C by thiol-specific reagents closed the spontaneously open channels. The leak current was reduced by MTSEA-biotin (2 mM; 57.2 ± 0.7%; $n = 3$), MTSEA-biotin-CAP (*N*-biotinylcaproylaminoethyl methanethiosulfonate) (2 mM; 63.0 ± 1.8%; $n = 3$), 2-aminoethyl methanethiosulfonate (MTSEA) (2 mM; 39.4 ± 1.4%; $n = 3$), MTSET (2-(trimethylammonium)ethyl methanethiosulfonate) (2 mM; 30.5 ± 0.9%; $n = 3$), and MTSES (2-sulfonatoethyl methanethiosulfonate) (2 mM; 26.8 ± 7.5%; $n = 3$) (Fig. 5). The observation that I_{leak} is reduced by tethering different chemical groups directly onto E155C suggests that this region of the binding site may play a key role in the triggering of allosteric transitions from the closed to open state.

MTSEA-biotin modification of cysteine residues

To further examine the β_2 subunit Ile^{154}–Asp^{163} region, we assessed the accessibility of cysteine residues introduced into this region. Wild-type and mutant receptors were exposed to MTSEA-biotin (2 mM; 2 min), a thiol-specific reagent that modifies water-accessible cysteine residues (Karlin and Akabas, 1998). MTSEA-biotin significantly reduced I_{GABA} for receptors containing E155C (91.8 ± 1.5%; $n = 6$), G158C (34.6 ± 4.5%; $n = 4$), T160C (60.9 ± 3.0%; $n = 10$), and D163C (98.9 ± 3.7%; $n = 8$) (Fig. 6). MTSEA-biotin had no effect on wild-type receptors or those containing I154C, S156C, T161C, and D162C. Lack of effect indicates that the thiol group was not accessible to modification or that modification produced no detectable functional effect. The accessibility pattern of the residues is consistent with the predicted side-chain positions observed in homology models of

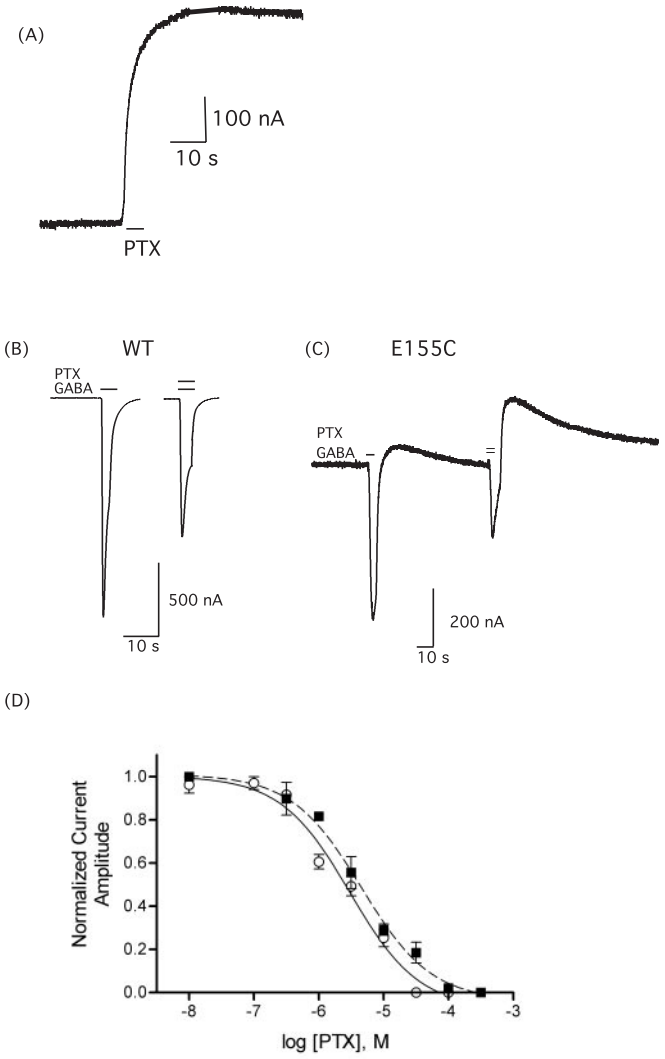

Figure 3. *A*, Representative current trace demonstrating that the high resting leak conductance for $\alpha_1\beta_2$(E155C) receptors expressed in *Xenopus* oocytes is sensitive to blockade by PTX (100 μM). PTX (100 μM) reduced the resting conductance (-609 ± 76 nA; $n = 9$) by $72.1 \pm 4.2\%$. Representative current traces obtained from PTX-mediated inhibition of GABA-evoked currents (EC_{50}) for wild-type (WT; *B*) and $\alpha_1\beta_2$(E155C) (*C*) receptors are shown. Note that the PTX IC_{50} value for the E155C mutant was determined by using the baseline leak current as the zero. *D*, Concentration dependence of PTX-mediated reduction of I_{GABA} (EC_{50}) current for wild type (■) and E155C (○) expressed in *Xenopus* oocytes. Data points represent the mean ± SE of three independent experiments. Data were normalized to I_{GABA} in the absence of PTX. IC_{50} values are summarized in Table 2.

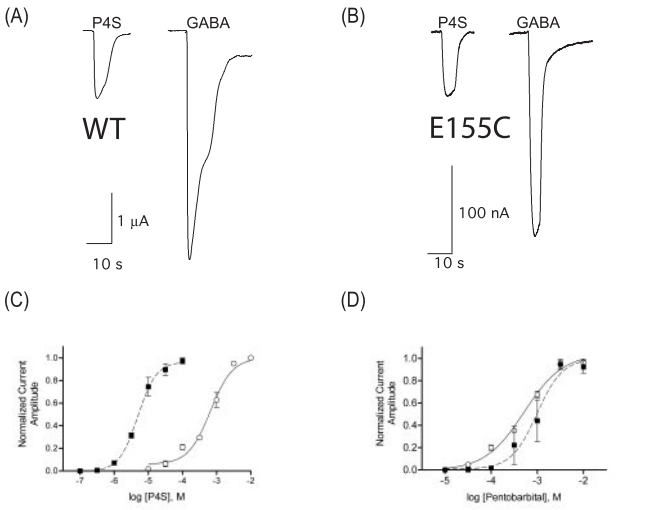

Figure 4. Representative current traces obtained from GABA- and P4S-mediated activation of wild-type (WT; *A*) and $\alpha_1\beta_2$(E155C) (*B*) receptors are shown. P4S efficacy at wild-type (0.41 ± 0.05; $n = 7$) and $\alpha_1\beta_2$(E155C) (0.47 ± 0.04; $n = 6$) receptors was not significantly different, where efficacy is reported as $I_{max\ P4S}/I_{max\ GABA}$. Values are given as mean ± SE. *C*, Concentration–response curves for P4S-activated current for wild-type (■) and $\alpha_1\beta_2$(E155C) (○) receptors expressed in *Xenopus* oocytes. *D*, Concentration–response curves for pentobarbital-activated current for wild-type (■) and $\alpha_1\beta_2$(E155C) (○) receptors. Data points represent the mean ± SE of three to four independent experiments. The EC_{50} values for P4S and pentobarbital are reported in Table 2.

the $GABA_A$ receptor, which envision this region of the $GABA_A$ receptor forming a loop structure (Cromer et al., 2002).

MTSEA-biotin rates of reaction

The rate of reaction of MTSEA-biotin with an introduced cysteine mainly depends on the ionization of the thiol group and the access route of the methanethiosulfonate reagent (Karlin and Akabas, 1998). Cysteine residues with ionized sulfhydryls react 10^8 to 10^9 times faster than nonionized sulfhydryls (Roberts et al., 1986). Second-order rate constants therefore provide information about the local environment of a substituted cysteine. The fast second-order rate constants (in the absence of other ligands) for MTSEA-biotin modification of D163C (604,771 $M^{-1}sec^{-1}$) and T160C (286,100 $M^{-1}sec^{-1}$) indicate that both residues are found in an open, aqueous environment. The second-order rate constant for E155C is significantly slower (27.9 $M^{-1}sec^{-1}$), suggesting that the thiol group is not well ionized and/or that the introduced cysteine residue is in a restricted–buried environment (Table 3, Fig. 7).

To determine whether a given residue lies near the neurotransmitter binding site, MTSEA-biotin reaction rates were measured in the presence of GABA and the competitive antagonist SR-95531. These ligands promote different conformational changes in the binding site (Boileau et al., 2002), and thus, if the rate at which MTSEA-biotin reacts with an introduced cysteine is slowed by both ligands, then it is likely that the ligands are sterically blocking the reaction and that the sulfhydryl side chain is facing into or near the GABA-binding site. Both GABA (at EC_{90} concentration) and SR-95531 (at IC_{90} concentration) significantly slowed modification of T160C and D163C approximately twofold (Fig. 8), suggesting that these residues are found within or near the GABA-binding site (Fig. 9). Although the data are consistent with GABA and SR-95531 causing a steric block, it is feasible that the binding of either ligand induces local allosteric changes in the receptor that leads to the slowing of MTSEA-biotin reaction rates. Neither ligand slowed modification of E155C (Table 3). Because α_1E155C receptors are spontaneously open, the control rate of MTSEA-biotin modification of E155C likely reflects reaction to a "ligand-bound, active" conformation of the binding site. Thus, the result that GABA and SR-95531 had no effect on modification rate is not surprising.

Effect of pentobarbital on MTSEA-biotin second-order rate constants

To identify whether movements occur in and near the Ile^{154}–Asp^{163} region of the GABA-binding site during channel gating and modulation, we measured the rates of reaction of MTSEA-biotin with T160C, D163C, and E155C in the presence pentobarbital. The ability of pentobarbital to alter the rates of modification provides an indirect measure of changes that occur within this

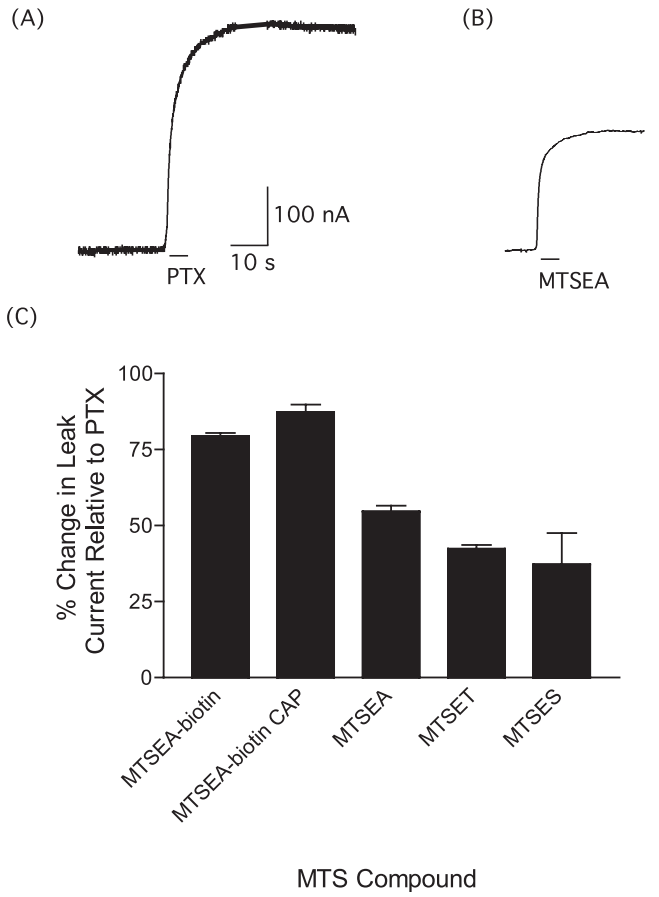

Figure 5. Representative traces demonstrating the effects of PTX (100 μM; *A*) and MTSEA (2 mM; *B*) on I_{leak} for $\alpha_1\beta_2$(E155C) receptors are shown. Reagents were applied in the absence of GABA and resulted in a reduction in the leak current. Note that the PTX trace is the same as that presented in Figure 3*A* but is included here for comparison purposes. *C*, Bar graph summarizing the effects of all methanethiosulfonate reagents on I_{leak}. Note that the maximum effect of each MTS reagent is normalized to the maximum effect obtained with 100 μM PTX for comparison purposes. The mean values for blockade of the resting conductance by MTS reagents are reported in Results. Error bars represent SE.

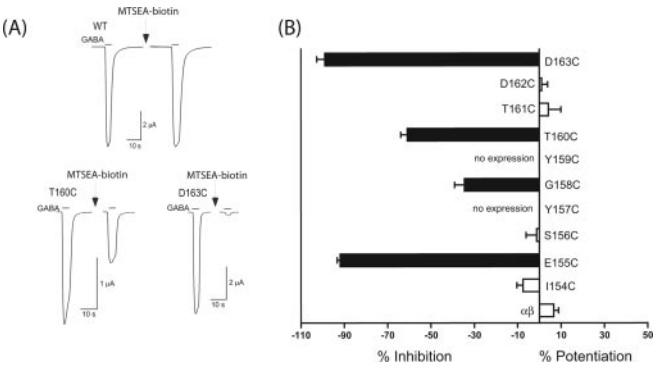

Figure 6. Summary of the effects of MTSEA-biotin (2 mM) on wild-type (WT) and mutant receptors. *A*, Representative current traces demonstrating the effects of MTSEA-biotin application on GABA-mediated current (EC_{50}) at wild-type and T160C- and D163C-containing receptors. The arrows in the current traces represent MTSEA-biotin application (2 min), and the breaks represent the subsequent wash (5 min). *B*, Summary of the effect of MTSEA-biotin at all receptors. The effect (percentage of inhibition or potentiation) is calculated using the following: $([I_{GABA\text{-}POST\ MTSEA\text{-}biotin}/I_{GABA\text{-}PRE\ MTSEA\text{-}biotin}] - 1) \times 100$. Bars represent the mean ± SE for 3–10 experiments. The filled bars indicate values that were statistically different from wild-type values ($*p < 0.001$). Note that expression of Y157C or Y159C failed to yield functional receptors.

region of the binding cleft in the transition from the resting to the active–desensitized states. As a result of the slowness of drug application using the oocyte expression system, we cannot easily determine whether the movement is associated with open or desensitized states. Nevertheless, coapplication of pentobarbital and MTSEA-biotin should capture receptor states that differ from that captured by application of MTSEA-biotin alone. Concentrations of pentobarbital (500 μM) that activate the receptor slowed the rate of MTSEA-biotin modification of T160C and D163C approximately twofold but had no effect on the second-order rate constant for E155C (Table 3). Thus, T160C and D163C act as reporters of barbiturate-mediated channel gating. Concentrations of pentobarbital that do not open the channel but potentiate GABA current (e.g., 50 μM) (Table 3) slowed modification of T160C but not D163C (Fig. 7*B*,*C*; Table 3). These data suggest that movements within the binding site associated with channel gating versus allosteric modulation are distinct.

Discussion

Binding-site movements that initiate ligand-gated ion channel activation are not well established. Here, we provide evidence that movement in the β_2 Ile^{154}–Asp^{163} region of the $GABA_AR$ is involved in coupling GABA binding to channel gating, and we describe a role for β_2Glu^{155} as an initial trigger for ion channel opening.

β_2 Ile^{154}–Asp^{163} mutations affect ligand binding and channel gating

If the β_2 Ile^{154}–Asp^{163} region plays a pivotal role for coupling binding to gating, one would expect that mutations within this domain would affect both processes. Seven cysteine substitutions significantly increase GABA EC_{50} values, which reflect changes in either microscopic binding affinity and/or channel gating (Colquhoun, 1998). Three of the seven mutations that shift the GABA EC_{50} (E155C, S156C, and G158C) also significantly reduce SR-95531 K_I, suggesting that at least one effect of these mutations is to alter ligand binding, because SR-95531 does not gate the channel (but see Ueno et al., 1997). $\alpha_1\beta_2$(G158C) and $\alpha_1\beta_2$(D163C) receptors have significantly reduced Hill coefficients for GABA activation, consistent with a reduction in gating efficacy (Colquhoun, 1998). β_2E155C results in spontaneously open $GABA_ARs$, clearly demonstrating that this mutation alters channel gating. In addition, expression of β_2E155C differentially shifts the concentration dependencies rightward for GABA, SR-95531, and P4S, indicating that the mutation also perturbs ligand binding (Zhang et al., 1994). Furthermore, tethering thiol-reactive groups onto β_2E155C closes the spontaneously open channels. Together, the data suggest that β_2Glu^{155} occupies a key position in the activation pathway involved in coupling ligand binding site to channel gating. Although detailed kinetic analyses of these mutations are required to quantitatively tease apart the effects of each of these mutations on microscopic binding affinity and channel gating properties, the above results indicate that mutations in β_2 Ile^{154}–Asp^{163} region of the GABA-binding site disrupt both affinity and efficacy.

Structural rearrangements during gating transitions

The β_2 subunit forms the principal side of the GABA-binding site. We conclude that β_2Asp^{163} and β_2Thr^{160} are found within or near the GABA-binding site, based on a slowing of the rate of MTSEA-biotin modification of T160C and D163C by both GABA and SR-95531. Protection by both ligands suggests steric hindrance of MTSEA-biotin modification, because agonists and

Table 3. Second-order rate constants for MTSEA-biotin-mediated modification of accessible engineered cysteine residues in the absence (control) and presence of SR-95531, GABA, and pentobarbital

	Control		SR-95531		GABA		Pentobarbital(500)		Pentobarbital(50)	
Receptor	k_2 ($M^{-1}sec^{-1}$)	*n*	k_2 ($M^{-1}sec^{-1}$)	*n*	k_2 ($M^{-1}sec^{-1}$)	*n*	k_2 ($M^{-1}sec^{-1}$)	*n*	k_2 ($M^{-1}sec^{-1}$)	*n*
$\alpha_1\beta_2$(E155C)	27.9 ± 11	3	24.8 ± 3.8	3	23.7 ± 3.7	3	27.5 ± 9.8	3	N.D.	
$\alpha_1\beta_2$(T160C)	288, 664 ± 24, 911	11	132, 200 ± 3, 524*	4	122, 828 ± 37, 753*	4	131, 768 ± 16, 610*	4	107, 493 ± 17, 751*	3
$\alpha_1\beta_2$(D163C)	604, 771 ± 22, 681	7	293, 200 ± 43, 267*	3	280, 018 ± 43, 416*	3	281, 760 ± 56, 625*	3	479, 100 ± 48, 932	4

Data represent the mean ± SE of 3–11 independent experiments (*n*). k_2 values were calculated by dividing the pseudo-first-order rate constant by the concentration of MTSEA-biotin used in the experiments. The concentrations of MTSEA-biotin used were 2 mM (E155C), 100 nM (T160C), and 50 nM (D163C). GABA ($5 \times EC_{50}$), SR-95531 ($6 \times K_I$), and pentobarbital (500 and 50 μM) were coapplied as described in Materials and Methods to determine their ability to alter the rate of covalent cysteine modification. N.D., Not determined. *$p < 0.01$; from control.

antagonists promote different conformational changes within the binding site (Armstrong and Gouaux, 2000). In addition, mutagenesis and homology modeling studies suggest that the β_2 Ile^{154}–Asp^{163} region lines part of the GABA-binding site (Amin and Weiss, 1993).

Tierney et al. (1996) predict that movements within the β_2 subunit are critical for channel gating. To test the hypothesis that the β_2 Ile^{154}–Asp^{163} region of the binding site undergoes structural rearrangements during channel activation, we measured the rate of MTSEA-biotin modification of introduced cysteines in the presence of pentobarbital (500 μM). Although the binding sites for GABA and pentobarbital differ, the final structure of the activated $GABA_A$ receptor channel is likely similar because both drugs produce similar single channel conductances (Jackson et al., 1982; Akk and Steinbach, 2000). We can therefore monitor pentobarbital-induced movements in the GABA-binding site during state transitions from resting to open–desensitized states. Coapplication of pentobarbital and MTSEA-biotin should capture this region of the receptor in a conformation that differs from that captured by application of MTSEA-biotin alone. The observation that pentobarbital significantly slows modification of T160C and D163C (approximately twofold) indicates that the environment surrounding these residues changes and that they are "conformationally sensitive" to channel activation, supporting our hypothesis that movements within this region are critical for channel gating. T160C also appears to act as a reporter for movements that occur during allosteric modulation, because the rate of MTSEA-biotin modification of T160C was slowed almost twofold in the presence of a low concentration of pentobarbital (50 μM) that potentiates but does not gate the channel.

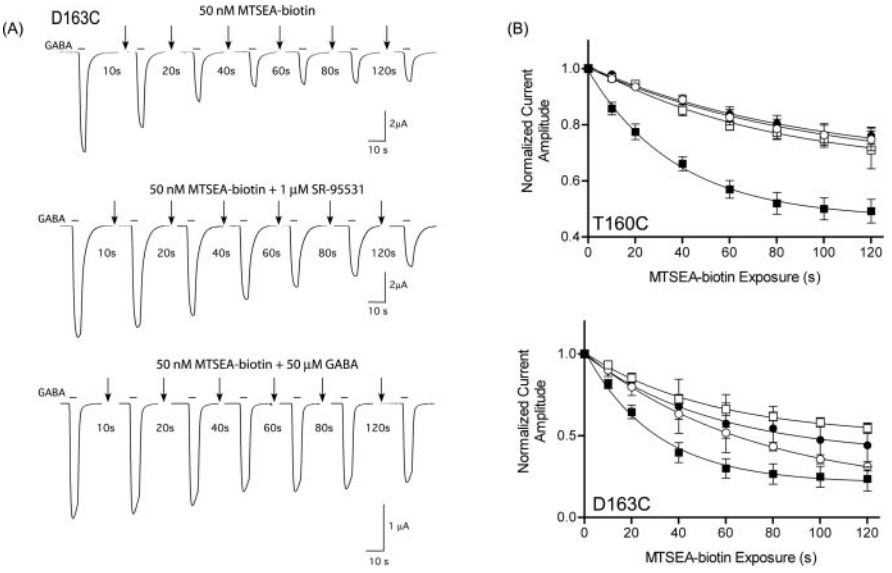

Figure 7. Rate of MTSEA-biotin modification of T160C and D163C. *A*, Representative GABA-evoked (EC_{50}) current traces after successive application (10–20 sec) of MTSEA-biotin on $\alpha_1\beta_2$(D163C) receptors in the absence or presence of SR-95531 ($6 \times K_I$) and GABA ($5 \times EC_{50}$). Sequential application of MTSEA-biotin reduced the amplitude of subsequent GABA-mediated (EC_{50}) currents at receptors containing T160C (*B*) and D163C (*C*). Data were normalized to the current measured at $t = 0$ for each experiment and plotted as a function of cumulative MTSEA-biotin exposure. Data were fitted to a single exponential function to get k_1. k_2 values were calculated by dividing the pseudo-first-order rate constant by the concentration of MTSEA-biotin used. Data points represent the mean ± SE for control (■), GABA (□), SR-95531 (○), and pentobarbital (500 μM; ●) for at least three independent experiments. Data are summarized in Table 3.

β_2 Ile^{154}–Asp^{163} is a protein hinge

Local agonist-induced movements within LGIC binding sites precede a conformational wave that leads to channel gating (Chakrapani et al., 2004). Structural studies suggest that the binding of ACh induces a 15° clockwise rotation of the inner β-sheets of the N-terminal ligand binding domain of the nAChR α_1 subunits. This, in turn, brings the $\beta1$-$\beta2$ loop (loop 2) into contact with the extracellular M2-M3 loop, and movement of the M2-M3 loop then causes the M2 region to rotate, which leads to opening of the channel gate (Miyazawa et al., 2003). Linear free energy analysis of the nAChR suggest that a conformational wave begins at the binding site and region A of the ACh-binding site (β-strand 4 and loop 5), followed by movements of loops 2, 7 (Cys-Cys loop) and the M2-M3 linker at the extracellular juxtapore region, and finally movement of the transmembrane domains (Grosman et al., 2000; Chakrapani et al., 2004). Studies examining the structural mechanisms of $GABA_AR$ activation have identified pairs of interacting residues within these regions that are necessary for coupling GABA binding to channel gating–desensitization. These include electrostatic interactions between negatively charged residues in loops 2 (α_1Asp^{57}) and 7 (α_1Asp^{149}) of the $GABA_AR$ and a positively charged lysine (α_1Lys^{279}) in the M2-M3 loop (Kash et al., 2003). Recently, a study using a chimeric receptor comprised of AChBP fused to the transmembrane pore domain of the 5-HT_{3A} receptor demonstrated that only when loops 2, 7, and 9 (region F of the binding site) from AChBP were replaced with 5-HT_{3A} receptor sequences did ACh binding trigger channel opening (Bouzat et al., 2004). This indicates that loops 2, 7, and 9 are critical elements involved in coupling the extracellular binding site domain to the transmembrane channel gating domain. During examination of homology models of the $GABA_AR$, we noticed that the β_2 Ile^{154}–Asp^{163} region of the binding site (β-strand 7 and loop 8) physically links loops 2 and 9. Thus, we speculate that the β_2

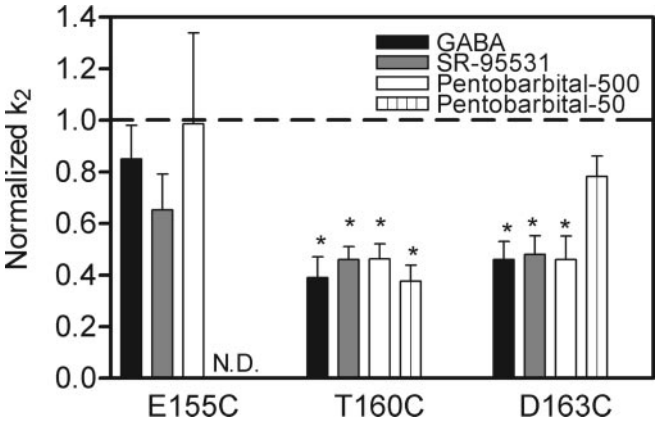

Figure 8. Summary of the effects of GABA, SR-95531, and pentobarbital on MTSEA-biotin second-order rate constants. Data were normalized to the control k_2 (rate measured when no other compound was present; denoted as a dashed line). Coapplication of GABA (5 x EC_{50}; black), SR-95531 (6 x K_I; gray), and pentobarbital [500 μM (white) or 50 μM (lined)] slows reaction of MTSEA-biotin at receptors carrying T160C and D163C (*$p < 0.001$; from control). Note that 50 μM pentobarbital significantly slows the rate of reaction at T160C but not at D163C. The ability of 50 μM pentobarbital to alter the rate of reaction at E155C was not determined (N.D.). Error bars represent SE.

Ile^{154}–Asp^{163} region may act as a protein hinge and that structural rearrangements within this region of the binding site could therefore be an efficient means for simultaneously propagating movements to both loops 2 and 9.

Movements in region B are also likely to be transmitted to the region C of the GABA-binding site (i.e., end of β-strand 9, loop 10 and beginning of β-strand 10). Based on homology models, possible interactions within regions B and C include the following amino acid pairs: β_2Glu^{153} and β_2Lys^{196}, β_2Glu^{155} and β_2Arg^{207}, as well as β_2Glu^{165} and β_2Lys^{197}. Previously, we demonstrated that β_2Arg^{207} stabilizes GABA binding (Wagner and Czajkowski, 2001; Wagner et al., 2004). We predict that the carboxylate side chain of Glu^{155} is within 2.5 Å from the guanido group of β_2Arg^{207} (Fig. 9) and may play a role in positioning the β_2Arg^{207} side chain. This may explain why mutation of β_2Glu^{155} disrupts orthosteric ligand binding. However, mutation of β_2Glu^{155} also produces spontaneously open channels and indicates that perturbation of this residue has additional long-range allosteric effects that are likely propagated to the channel gate by changes in the positions of regions B and C located in the binding site as well as loops 2 and 9 near the juxtapore region. Additional experiments are needed to test these hypotheses. Support for interactions between regions B and C of LGIC binding sites comes from studies of the nAChR. It has been reported that a hydrogen bond between a residue in region B (G152K) and in region C (P193I) of the nAChR α_7 subunit is important for nAChR activation (Grutter et al., 2003) and may serve to explain how the α_1G153S human polymorphism gives rise to a slow channel myasthenic syndrome (Sine et al., 1995).

Finally, the β_2 Ile^{154}–Asp^{163} region may also be involved in intersubunit interactions. Models of the N-terminal domains of $GABA_AR$ predict that β_2Asp^{163} forms a salt bridge with α_1Arg^{119} and β_2Arg^{28}. The roles of salt bridges in $GABA_AR$ function are not presently known, but it is believed that salt bridges may limit the number of conformations of a protein complex, be key participants in determining ligand binding geometry, or be important for the association of subunits in multiprotein complexes (Hendsch and Tidor, 1994). The disruption or formation of bonds among these charged residues at subunit interfaces may be

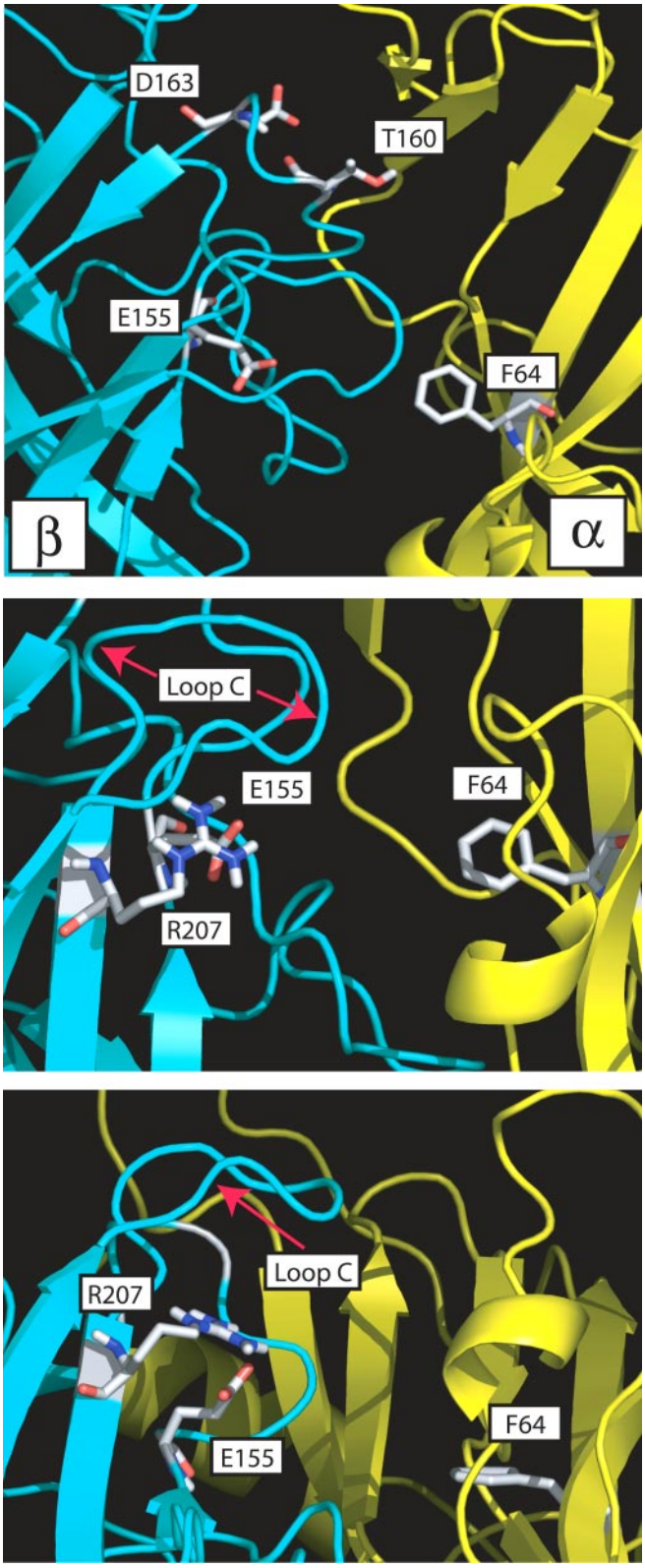

Figure 9. Top, Side view of a homology model of the GABA-binding site β (cyan)-α (yellow) subunit interface with residues β_2Glu^{155}, β_2Thr^{160}, β_2Asp^{163} in region B and residue α_1Phe^{64} in region D displayed as sticks. Middle, Position of β_2Glu^{155} (region B) relative to β_2Arg^{207} (region C) is highlighted. β_2Arg^{207} has been identified previously as a GABA-binding site residue (Wagner and Czajkowski, 2001; Wagner et al., 2004). Bottom, View of the binding site from below, which shows the close apposition of β_2Glu^{155} and β_2Arg^{207} (2.5 Å), suggesting an electrostatic interaction between the two residues.

important for conformational changes that occur during activation and/or desensitization. Mutation of β_2Asp^{163} significantly decreased the Hill coefficient for GABA activation of the receptor and is consistent with this hypothesis.

Conclusions

The β_2 Ile^{154}–Asp^{163} region of the $GABA_A$R-binding site appears to be a protein hinge that is uniquely positioned to transduce binding site movements to the cascade of events that lead to opening of the ion channel. We demonstrate that the region undergoes conformational rearrangements during pentobarbital-mediated gating events, and mutation of β_2Glu^{155} gives rise to spontaneously open channels, suggesting that movements in this region of the GABA-binding site are one of the initial triggers for coupling binding to gating. Ultimately, precise mapping of interresidue contacts will be required to test this activation mechanism and to define the pathway leading from the binding site to the channel gate.

References

Akk G, Steinbach JH (2000) Activation and block of recombinant $GABA_A$ receptors by pentobarbitone: a single-channel study. Br J Pharmacol 130:249–258.

Amin J, Weiss DS (1993) $GABA_A$ receptor needs two homologous domains of the β-subunit for activation by GABA but not by pentobarbital. Nature 366:565–569.

Armstrong N, Gouaux E (2000) Mechanisms of activation and antagonism of an AMPA-sensitive glutamate receptor: crystal structures of the GluR2 ligand binding core. Neuron 28:165–181.

Baumann SW, Baur R, Sigel E (2001) Subunit arrangement of γ-aminobutyric acid type A receptors. J Biol Chem 276:36275–36280.

Baumann SW, Baur R, Sigel E (2002) Forced subunit assembly in $\alpha_1\beta_2\gamma_2$ $GABA_A$ receptors: insight into the absolute arrangement. J Biol Chem 277:46020–46025.

Bertrand D, Devillers-Thiéry A, Revah F, Galzi JL, Hussy N, Mulle C, Bertrand S, Ballivet M, Changeux JP (1992) Unconventional pharmacology of a neuronal nicotinic receptor mutated in the channel domain. Proc Natl Acad Sci USA 89:1261–1265.

Boileau AJ, Kucken AM, Evers AM, Czajkowski C (1998) Molecular dissection of benzodiazepine binding and allosteric coupling using chimeric γ-aminobutyric $acid_A$ receptor subunits. Mol Pharmacol 53:295–303.

Boileau AJ, Evers AM, Davis AF, Czajkowski C (1999) Mapping the agonist binding site of the $GABA_A$ receptor: evidence for a β-strand. J Neurosci 19:4847–4854.

Boileau AJ, Newell JG, Czajkowksi C (2002) $GABA_A$ receptor β_2Tyr^{97} and Leu^{99} line the GABA-binding site: insights into the mechanisms of agonist and antagonist actions. J Biol Chem 277:2931–2937.

Bouzat C, Gumilar F, Spitzmaul G, Wang HL, Rayes D, Hansen SB, Taylor P, Sine SM (2004) Coupling agonist binding to channel opening in an ACh-binding protein linked to an ion channel. Nature 430:896–900.

Brejc K, van Dijk W, Klaassen RV, Schuurmans M, van der Gost J, Smit AB, Sixma T (2001) Crystal structure of an ACh-binding protein reveals the ligand-binding domain of nicotinic receptors. Nature 17:269–276.

Chakrapani S, Bailey TD, Auerbach A (2004) Gating dynamics of the acetylcholine receptor extracellular domain. J Gen Physiol 123:341–356.

Chang Y, Weiss DS (1998) Substitution of the highly conserved M2 leucine create spontaneously opening ρ1 γ-aminobutyric acid receptors. Mol Pharmacol 53:511–523.

Chang Y, Weiss DS (1999) Allosteric activation mechanism of the $\alpha1\beta2\gamma2$ γ-aminobutyric acid type A receptor revealed by mutation of the conserved M2 leucine. Biophys J 77:2543–2551.

Chang Y, Weiss DS (2002) Site-specific fluorescence reveals distinct structural changes with GABA receptor activation and antagonism. Nat Neurosci 5:1163–1168.

Chang Y, Wang R, Barot S, Weiss DS (1996) Stoichiometry of a recombinant $GABA_A$ receptor. J Neurosci 16:5415–5424.

Cheng Y, Prussof WH (1973) Relationship between the inhibition constant (KI) and the concentration of inhibitor which causes 50 percent inhibition (I50) of an enzymatic reaction. Biochem Pharmacol 22:3099–3108.

Colquhoun D (1998) Binding, gating, affinity and efficacy: the interpretation of structure-activity relationships for agonists and the effects of mutating receptors. Br J Pharmacol 125:924–927.

Cromer BA, Morton CJ, Parker MW (2002) Anxiety over $GABA_A$ receptor structure relieved by AChBP. Trends Biochem Sci 27:280–287.

Croxen R, Newland C, Beeson D, Oosterhuis H, Chauplannaz G, Vincent A, Newsom-Davis J (1997) Mutations in different functional domains of the human muscle acetylcholine receptor α subunit in patients with slow-channel myasthenia gravis. Hum Mol Genet 6:767–774.

Daniels GM, Amara S (1998) Selective labeling of neurotransmitter transporters at the cell surface. Methods Enzymol 296:307–318.

Dennis M, Giraudat J, Kotzyba-Hibert F, Goeldner M, Hirth C, Chang JY, Lazure C, Chrétien M, Changeux JP (1988) Amino acids of the *Torpedo marmorata* acetylcholine receptor α subunit labeled by a photoaffinity ligand for the acetylcholine binding site. Biochemistry 27:2346–2357.

Farrar SJ, Whiting PJ, Bonnert TP, McKernan RM (1999) Stoichiometry of a ligand-gated ion channel determined by fluorescence energy transfer. J Biol Chem 274:10100–10104.

Filatov GN, White MW (1995) The role of leucine residues in the M2 domain of the acetylcholine receptor in channel gating. Mol Pharmacol 48:379–384.

Findlay G, Ueno S, Harrison NL, Harris RA (2000) Allosteric modulation in spontaneously active mutant γ-aminobutryic $acid_A$ receptors in frogs. Neurosci Lett 293:155–158.

Galzi JL, Changeux JP (1994) Neurotransmitter-gated ion channels as unconventional allosteric proteins. Curr Opin Struct Biol 4:554–565.

Galzi JL, Revah F, Black D, Goeldner M, Hirth C, Changeux JL (1991) Identification of a novel amino acid α-tyrosine 93 within the cholinergic ligands-binding sites of the acetylcholine receptor by photoaffinity labeling: additional evidence for a three-loop model of the cholinergic ligands-binding sites J Biol Chem 265:10430–10437.

Grosman C, Zhou M, Auerbach A (2000) Mapping the conformational wave of acetylcholine receptor gating. Nature 403:773–776.

Grutter T, de Carvalho LP, Le Novère N, Corringer PJ, Edelstein S, Changeux JP (2003) An H-bond between two residues from different loops of the acetylcholine binding site contributes to the activation mechanism of nicotinic receptors. EMBO J 22:1990–2003.

Hendsch SB, Tidor B (1994) So salt bridges stabilize proteins? A continuum electrostatic analysis. Protein Sci 3:211–226.

Holden JH, Czajkowski C (2002) Different residues in the $GABA_A$ receptor α_1T60-α_1K70 region mediate GABA and SR-95531 actions. J Biol Chem 277:18785–18792.

Horenstein J, Wagner DA, Czajkowksi C, Akabas MH (2001) Protein mobility and GABA-induced conformational changes in the $GABA_A$ receptor pore-lining M2 segment. Nat Neurosci 4:477–485.

Im WB, Pregenzer JF, Binder JA, Dillon GH, Alberts GL (1995) Chloride channel expression with the tandem construct of α6-β2 $GABA_A$ receptor subunit requires a monomeric subunit of α6 or γ2. J Biol Chem 270:26063–26066.

Jackson MB, Lecar H, Matthers D, Barker JL (1982) Single channel currents activated by gamma-aminobutyric acid, muscimol and (−)pentobarbital in cultured mouse spinal neurons. J Neurosci 2:889–894.

Karlin A, Akabas M (1998) Substituted-cysteine accessibility method. Methods Enzymol 293:123–145.

Kash TL, Jenkins A, Kelley JC, Trudell JR, Harrison NL (2003) Coupling of agonist binding to channel gating in the $GABA_A$ receptor. Nature 42:272–275.

Kucken AM, Wagner DA, Ward PH, Teissére JA, Boileau AJ, Czajkowski C (2000) Identification of benzodiazepine binding site residues in the γ2 subunit of the γ-aminobutyric $acid_A$ receptor. Mol Pharmacol 57:932–939.

Labarca C, Nowak MW, Zhang H, Tang L, Despande P, Lester HA (1995) Channel gating governed symmetrically by conserved leucine residues in the M2 domain of nicotinic receptors. Nature 376:514–516.

LeNovère N, Grutter T, Changeux JP (2002) Models of the extracellular domain of the nicotinic receptors and of agonist- and Ca^{2+}-binding sites. Proc Natl Acad Sci USA 99:3210–3215.

Lester HA, Dibas MI, Dahan DS, Leite JF, Dougherty DA (2004) Cys-loop receptors: new twists and turns. Trends Neurosci 27:329–336.

Liman ER, Tygat J, Hess P (1992) Subunit stoichiometry of a mammalian K^+ channel determined by construction of multimeric cDNAs. Neuron 9:861–871.

Miyazawa A, Fujiyoshi Y, Unwin N (2003) Structure and gating mechanism of the acetylcholine receptor pore. Nature 423:949–955.

Newell JG, Czajkowski C (2003) The $GABA_A$ receptor $\alpha 1$ subunit Pro^{174}-Asp^{191} segment is involved in GABA binding and channel gating. J Biol Chem 278:13166–13172.

Pascual JM, Karlin A (1998) State-dependent accessibility and electrostatic potential in the channel of the acetylcholine receptor: inferences from rates of reaction of thiosulfonates with substituted cysteines in the M2 segment of the α subunit. J Gen Physiol 111:717–739.

Powell JMD (1977) Restart procedures for the conjugate gradient method. Math Program 12:241–251.

Press WH, Flannery BP, Teukolsky SA, Vetterling WT (1988) Numerical recipes in C: the art of scientific computing. In: Minimization and maximization of functions, Ed 1, Chap 10, pp 301–327. Cambridge, UK: Cambridge UP.

Pritchett DB, Sontheimer H, Shivers DB, Ymer S, Kettenham H, Schofield PR, Seeburg PH (1989) Importance of a novel $GABA_A$ receptor subunit for benzodiazepine pharmacology. Nature 338:582–585.

Reeves DC, Sayed MF, Chau PL, Price KL, Lummis SC (2003) Prediction of $5\text{-}HT_3$ receptor agonist-binding residues using homology modeling. Biophys J 84:2338–2344.

Roberts DD, Lewis SD, Ballou DP, Olson ST, Shafer JA (1986) Reactivity of small thiolate anions and cysteine-25 in papain toward methyl methanethiosulfonate. Biochemistry 25:5595–5601.

Robertson GA, Warmke JM, Ganetzky B (1996) Potassium currents expressed from *Drosophila* and mouse eag cDNAs in *Xenopus* oocytes. Neuropharmacology 35:841–850.

Schmieden V, Kuhse J, Betz H (1993) Mutation of glycine receptor subunit creates β-alanine receptor responsive to GABA. Science 262:256–258.

Schofield PR, Darlison MG, Fujita N, Burt DR, Stephenson FA, Rodriguez H, Rhee LM, Ramachandran J, Reale V, Glencorse TA (1987) Sequence identity and functional expression of the GABA-A receptor shows a ligand-gated receptor super-family. Nature 328:221–227.

Sine S, Ohno K, Bouzat C, Auerbach A., Milone M, Pruit JN, Engel G (1995) Mutation of the acetylcholine receptor subunit causes a slow-channel myasthenic syndrome by enhancing agonist binding affinity. Neuron 15:229–239.

Spier AD, Lummis SC (2000) The role of tryptophan residues in the $5\text{-hydroxytryptamine}_3$ receptor ligand binding domain. J Biol Chem 275:5620–5625.

Sugiyama N, Boyd AE, Taylor P (1996) Anionic residue in the α-subunit of the nicotinic acetylcholine receptor contributing to subunit assembly and ligand binding. J Biol Chem 271:26575–26581.

Thompson SA, Smith MZ, Wingrove PB, Whiting PJ, Wafford KA (1999) Mutation at the putative GABAA ion-channel gate reveals changes in allosteric modulation. Br J Pharmacol 127:1349–1358.

Tierney ML, Birnir B, Pillai NP, Clements JD, Howitt SM, Cox GB, Gage PW (1996) Effects of mutating leucine to threonine in the M2 segment of the α_1 and β_1 subunits of the $GABA_A$ $\alpha_1\beta_1$ receptors. J Membr Biol 154:11–21.

Torres VI, Weiss DS (2002) Identification of a tyrosine in the agonist binding site of the homomeric $\rho 1$ γ-aminobutyric acid (GABA) receptor that, when mutated, produces spontaneous opening. J Biol Chem 277:43741–43748.

Tretter V, Ehya N, Fuchs K, Sieghart W (1997) Stoichiometry and assembly of a recombinant $GABA_A$ receptor subtype. J Neurosci 17:2728–2737.

Ueno S, Bracamontes J, Zorumski C, Weiss DS, Steinbach JH (1997) Bicuculline and gabazine are allosteric inhibitors of channel opening of the $GABA_A$ receptor. J Neurosci 17:625–634.

Unwin N, Miyazawa A, Li J, Fujiyoshi Y (2002) Activation of the nicotinic acetylcholine receptors involves a switch in conformation of α subunits. J Mol Biol 319:1165–1176.

Vandenberg RJ, French CR, Barry PH, Shine J, Schofield PR (1992) Antagonism of ligand-gated ion channel receptors: two domains of the glycine receptor α subunit form the strychnine-binding site. Proc Natl Acad Sci USA 89:1765–1769.

Vandenberg RJ, Rajendra S, French CR, Barry PH, Schofield SC (1993) The extracellular disulfide loop motif of the inhibitory glycine receptor α subunit forms the strychnine-binding site. Mol Pharmacol 44:198–203.

Wagner DA, Czajkowski C (2001) Structure and dynamics of the GABA binding pocket: a narrowing cleft that constricts during channel activation. J Neurosci 21:67–74.

Wagner DA, Czajkowski C, Jones MV (2004) An arginine involved in GABA binding and unbinding but not gating of the $GABA_A$ receptor. J Neurosci 24:2733–2741.

Zhang HG, ffrench-Constant RH, Jackson M (1994) A unique amino acid of the *Drosophila* GABA receptor with influence on drug sensitivity by two mechanisms. J Physiol (Lond) 479:65–75.